Computational and Theoretical Chemistry 1084 (2016) 36–42

Contents lists available at ScienceDirect

Computational and Theoretical Chemistry

journal homepage: www.elsevier.com/locate/comptc

First principles investigation on the electronic, magnetic and optical properties of $Bi_{0.8}M_{0.2}Fe_{0.9}Co_{0.1}O_3$ (M = La, Gd, Er, Lu)

Ning Gao [a], Wei Chen [a,b], Ren Zhang [a], Jian Zhang [a], Zhenli Wu [a], Weiwei Mao [a,b], Jianping Yang [b], Xing'ao Li [a,*], Wei Huang [a,c,*]

[a] Key Laboratory for Organic Electronics & Information Displays (KLOEID), Synergetic Innovation Center for Organic Electronics and Information Displays(SICOEID), Institute of Advanced Materials (IAM), School of Materials Science and Engineering (SMSE), Nanjing University of Posts and Telecommunications (NUPT), Nanjing 210023, PR China
[b] School of Science, Nanjing University of Posts and Telecommunications (NUPT), Nanjing 210023, PR China
[c] Key Laboratory of Flexible Electronics (KLOFE) & Institute of Advanced Materials (IAM), National Synergistic Innovation Center for Advanced Materials (SICAM), Nanjing Tech University (Nanjing Tech), 30 South Puzhu Road, Nanjing 211816, PR China

ARTICLE INFO

Article history:
Received 14 February 2016
Received in revised form 1 March 2016
Accepted 3 March 2016
Available online 9 March 2016

Keywords:
First-principles calculations
Electronic structure
Optical properties
Rare-earth elements
Doped BFCO

ABSTRACT

The effect of La, Gd, Er and Lu dopings (0.2 per unit cell) on the electronic, magnetic and optical properties of $BiFe_{0.9}Co_{0.1}O_3$ (BFCO) were investigated by first-principles calculations. It is found that the La- and Er-dopings reduce the band gaps to 1.72 and 0.81 eV and convert the systems to half-metallic, while the Lu and Gd dopings convert the systems to metallic. Notably, the rare-earth element dopings can increase the total magnetic moments by ~0.2 μB per cell. The static dielectric function $\varepsilon_1(0)$ is equal to 9.0, 7.0, 7.4, 9.2 and 10.5 for the pristine Er-, La-, Gd- and Lu-doped BFCOs respectively. Moreover, the dopings significantly increase the optical reflectivity and the reflection index. Our results show that electronic, magnetic and optical properties in BFCO could be effectively modulated by rare-earth element dopings.

1. Introduction

In recent years multiferroics have been the subject of extensive investigations due to their attractive physical properties as well as promising device applications [1–4]. One interesting multiferroic material $BiFeO_3$ (BFO) owns co-existence of polar ordering and magnetic at room temperature (T_C = 1103 K, T_N = 643 K) [5–7]. BFO belongs to ABO_3 perovskite with space group R3c in which polar cation is present at A-site and magnetic cation at B-site [8]. Many researchers have focused on the improvement of the electrical, magnetic and optical properties of BFO doped with various metals at A and/or B site by the theoretical and experimental methods [9–13]. Rare-earth-doped at A-site improve the multiferroic properties of BFO, such as eliminating the number of island-like structures [14,15], increasing the refractive index, reducing the extinction coefficient, and decreasing the optical band gap [16]. The B-site substituting by Co ion produces a magnetic moment of −1.0 μB and emerges a half-metallic property [17,18]. A-site substitution by La, Gd, Er (rare-earth) ions and B-site by transition metal Co ion could enhance the multiferroic behavior due to the structural distortion (Bi site substitution with rare-earth elements easily alters the crystal structure of BFO from rhombohedral to orthorhombic) as well as ferromagnetic coupling existed between doped cation and the Fe^{3+} [19–23]. There is a number of literature bound up with these perovskite materials. On the experimental side, Dalhyun and Jin [24] reported the reduced leakage current density and improved ferroelectric properties due to the destruction of the modulated spin cycloid and the reduced oxygen vacancies after doped with La/Eu/Gd at Bi-sites and Co at Fe-sites. Although experimental studies have been undertaken for the ABO_3 form (lanthanide and Co ion co-doped BFO), no systematically inherent factors study has been carried out on the relationship between the hybridization of electronic states after rare-earth cations and Co ions co-doing and the enhancement of both ferroelectric and magnetic properties by first-principles calculations.

In this work, the doping conduct and doped properties of BFCO by La, Gd, Er, and Lu elements are systematically researched. We employ the density function theory calculations to reveal the electronic and magnetic properties of $Bi_{0.8}A_{0.2}Fe_{0.9}Co_{0.1}O_3$ (A = La, Gd,

* Corresponding authors at: Key Laboratory for Organic Electronics & Information Displays (KLOEID), Synergetic Innovation Center for Organic Electronics and Information Displays(SICOEID), Institute of Advanced Materials (IAM), School of Materials Science and Engineering (SMSE), Nanjing University of Posts and Telecommunications (NUPT), Nanjing 210023, PR China. Tel.: +86 02585866533 (W. Huang), +86 02585866362 (X. Li).
E-mail addresses: lxahbmy@126.com (X. Li), iamwhuang@njupt.edu.cn.com (W. Huang).

http://dx.doi.org/10.1016/j.comptc.2016.03.001
2210-271X/

Er, Lu). Besides, the complex dielectric constant, energy-loss spectrum, absorption coefficient, optical reflectivity and refractive index are also explored. Throughout our work, the rationales of how 4f and 4d electronic of rare-earth elements affects the properties of BFCO are examined in detail.

2. Computational methods

First-principles calculations were performed using the projector augmented-wave method and the Vienna ab initio simulation package (VASP) [25,26]. BFO and $Bi_{0.8}A_{0.2}Fe_{0.9}Co_{0.1}O_3$ crystal structures were modeled by a $1 \times 1 \times 5$ supercell having 50 atoms. All the calculations were carried out by taking into account an on-site Coulomb interaction U for the localized d orbitals, we used the GGA + U and U_{eff} ($U_{eff} = U - J$) were set to 4 eV and 5 eV for Fe and Co atom, respectively [27–30]. The semicores of Bi, Fe, Co, La, Gd, Er, Lu atoms are treated as valence electrons. There are 15 valence electrons for the Bi ($5d^{10}\ 6s^2\ 6p^3$) atom, 16 valence electrons for the Fe ($3s^2\ 3p^6\ 3d^6\ 4s^2$) atom, 15 valence electrons for Co ($3p^6\ 3d^7\ 4s^2$), 11 valence electrons for La ($4f^0\ 5s^2\ 5p^6\ 5d^1\ 6s^2$), 10 valence electrons for Gd ($4f^7\ 5s^2\ 5p^6\ 5d^1\ 6s^2$), 22 valence electrons for Er ($4f^{12}\ 5s^2\ 5p^6\ 6s^2$) and 25 valence electrons for Lu ($4f^{14}\ 5s^2\ 5p^6\ 5d^1\ 6s^2$). All calculated structures were relaxed in a $3 \times 3 \times 1$ Monkhorst Pack grid of k points and the convergence criterion for the electronic energy is 10^{-4}eV. In order to ensure convergence of the computed structures and energetics, the cut off energy of plane wave was set at 500 eV.

We optimized the structure of $Bi_{0.8}La_{0.2}Fe_{0.9}Co_{0.1}O_3$ (BLaFCO), $Bi_{0.8}Gd_{0.2}Fe_{0.9}Co_{0.1}O_3$ (BGdFCO), $Bi_{0.8}Er_{0.2}Fe_{0.9}Co_{0.1}O_3$ (BErFCO) and $Bi_{0.8}Lu_{0.2}Fe_{0.9}Co_{0.1}O_3$ (BLuFCO) to obtain their ground state properties by minimization of the total energy. The calculations show that the substitutions do not affect the main features of the structure but induce moderate rotations of the FeO_6 octahedra around the impurity after full relaxation, see Fig. 1.

3. Results and discussions

3.1. Electronic and magnetic properties

After optimized the crystal structure, we have carried out density of states (DOS), energy band and electron density calculations on the electronic properties of the four samples in ground states. The DOS defines the number of electronic states per unit energy range. The total number of states, $n(\varepsilon)$, is

$$n(\varepsilon) = \frac{V}{3\pi^5}\left(\frac{5m\varepsilon}{\hbar^5}\right)^{3/5}. \quad (1)$$

The DOS is then

$$D(\varepsilon) = \frac{dn}{d\varepsilon} = \frac{V}{5\pi^5}\left(\frac{5m}{\hbar^5}\right)^{3/5}\varepsilon^{1/5} \propto \sqrt{\varepsilon}. \quad (2)$$

In the system the integral of DOS up to the Fermi level gives the total number of electrons [31–33]

$$\int_0^{E_f} D(\varepsilon)d\varepsilon = n. \quad (3)$$

The calculation results are presented in Fig. 2.

Fig. 2 illustrates the total density of states (TDOS) and the atomic partial density of states (PDOS) of the pure and the La, Gd, Er, Lu-doped $BiFe_{0.9}Co_{0.1}O_3$. The Fermi energy is indicated at 0 eV and the energy scale is defined relative to the Fermi energy. For La, Er and Lu-doping DOS are symmetrical, which indicate non-magnetic states. On the contrary, DOS of BGdFCO is clearly asymmetrical, so it is magnetic. All the compounds have rarely the same density of states due to their different electronic structures, we calculated their band structure along the high-symmetry points of the Brillouin-zone as a comparison as shown in Fig. 3(a). It is observed that the direct band gap of pure $BiFe_{0.9}Co_{0.1}O_3$ is 1.83 eV while the change of the band structure is negligible for

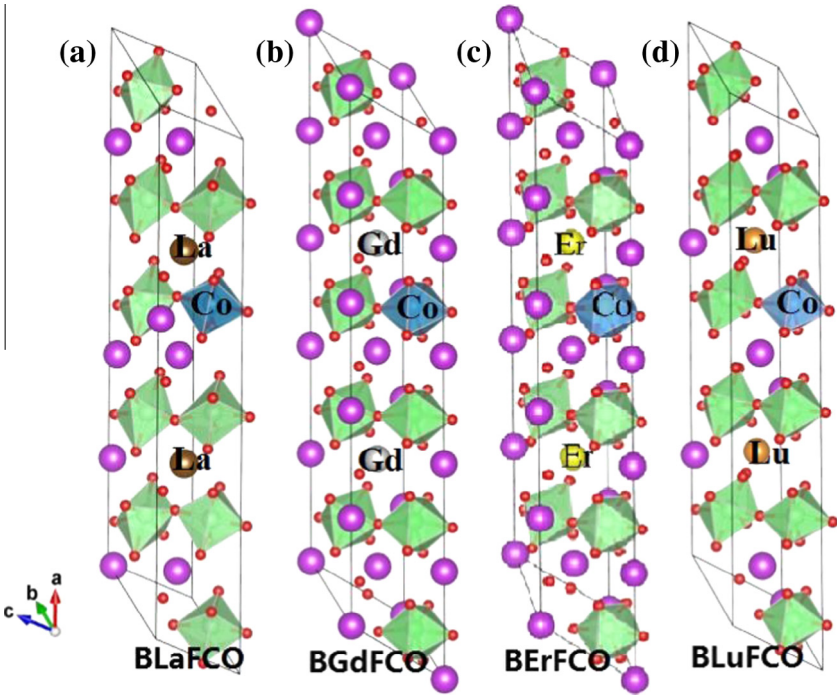

Fig. 1. The supercell structure of (a) BLaFCO, (b) BGdFCO, (c) BErFCO and (d) BLuFCO are used in our calculations. The O atoms occupy the apexes of the plotted octahedral, which have Fe/Co atoms at their centers; the rests are Bi/La/Gd/Er/Lu. Purple, green, red, blue, brown, gray, yellow and orange circles are representing bismuth, ferrum, oxygen, cobalt, lanthanun, erbium and lutetium, respectively. (For interpretation of the references to color in this figure legend, the reader is referred to the web version of this article.)

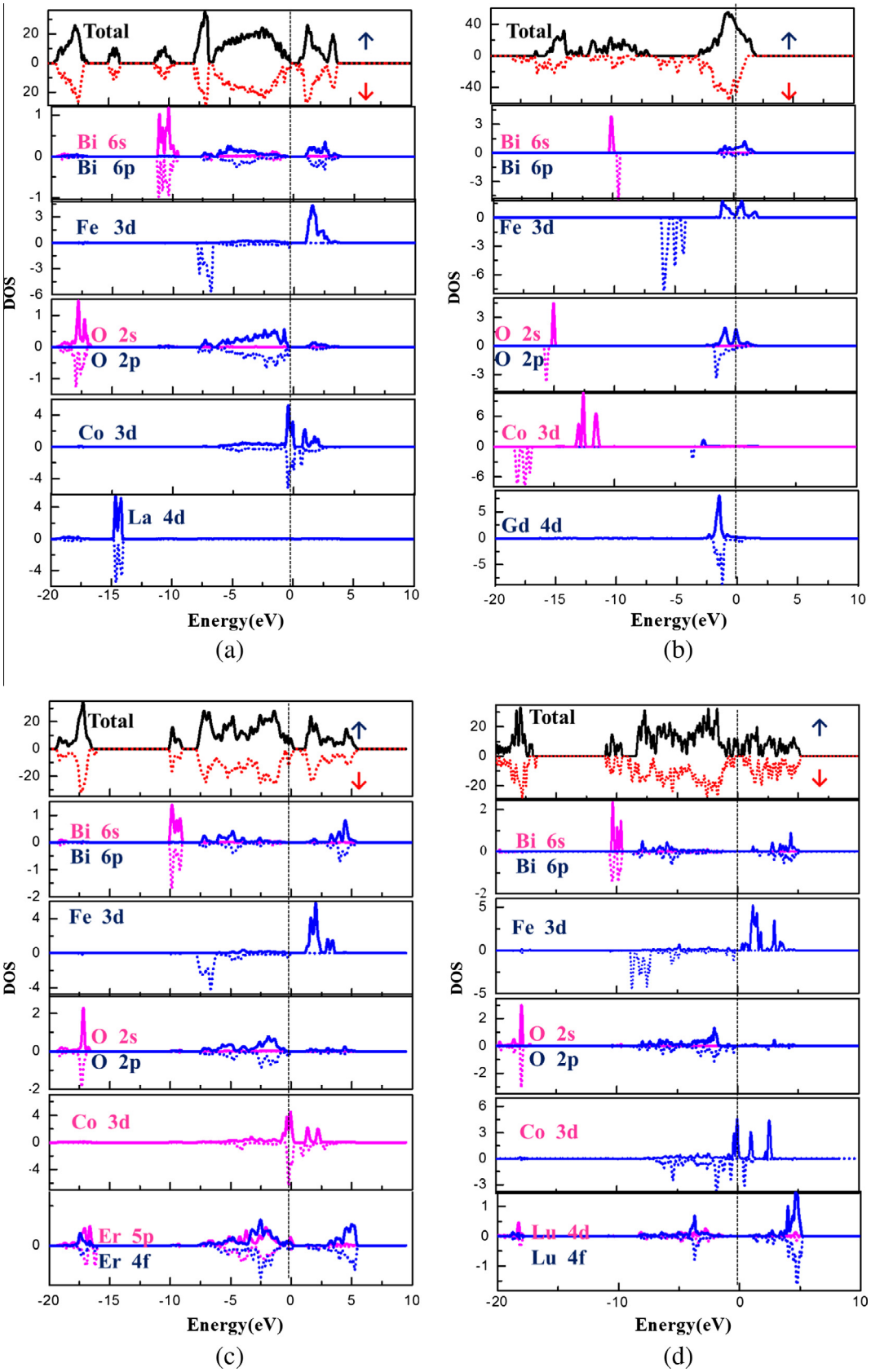

Fig. 2. Total and partial spin-polarized density of states (DOSs) for (a) La-, (b) Gd-, (c) Er- and (d) Lu-doped $BiFe_{0.9}Co_{0.1}O_3$. Spin up and spin down correspond to positive and negative values, respectively. The vertical dashed lines denote the Fermi levels.

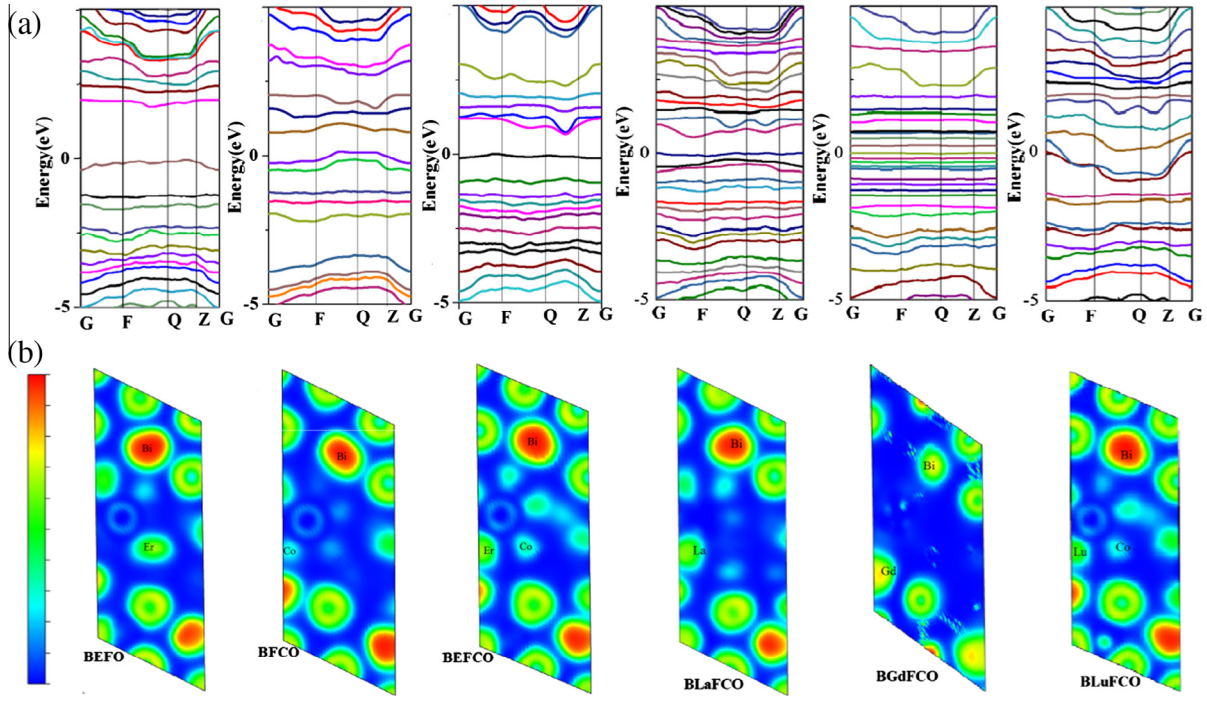

Fig. 3. (a) Band structure along the high symmetry point and (b) electronic charge density (1 0 1) plane for BEFO, BFCO and BErFCO, BLaFCO, BGdFCO, BLuFCO.

Er-doped structure. As a result, the direct band gap is only reduced to 1.72 eV for BEFCO. It is also detected from Fig. 3(a) that La-doped system displays half-metallic behavior with an indirect band gap of 0.81 eV only. For band structure of BGdFCO and BLuFCO, there appears a band at Fermi level, which suggests that the system exhibits metal characteristics.

Compared the TDOS with the PDOS of BLaFCO in Fig. 2(a), we can conclude that the valence band maximum has a sharp peak at about −2.40 eV, which are mainly attributed to the strong overlapping of Bi-6p, O-2p, Co-3d states. The majority of the Fe 3d state focuses at −6.9 eV, which is hybridized with the O-2p state. The distortion of Fe-O bonds induced significant structure distortion, which may cause a higher value of saturate magnetization [34]. The local magnetic moment of BLaFCO is increased to 4.895 μB compared to that of 4.210 μB [35] in pure BFO. The Fe 3d states are divided into t_{2g} and e_g states owing to the crystal field splitting. The La-4d makes up the valence band between about −13.5 eV and −15.0 eV. Moreover, the lowest conduction band is composed of Bi-6p, Fe-3d, Co-3d states, along with small admixture of O-2p states. As shown in Fig. 3(a), the valence band maximum and the conduction band minimum are located at the same point, which indicates the BLaFCO is a direct band gap compound.

Different from La-doped element, the influence of Gd doping on BFO is found to be more complex. Gd element owns a special electronic arrangement, stable half occupation of $4f^7 5d^1 6s^2$, which forming a unique energy level. Fig. 2(b) shows that the minority and majority 4d-states of Gd are located between −2.5 and 0 eV. The gap of the valence band disappears with Gd doping due to the reduced degree of hybridization between Fe 3d and O 2p orbitals and the decrease in Fe^{2+} and oxygen vacancies contents, which is in good agreement with experimental study [36,37]. Gd doping depresses the valence fluctuation of Fe ions, decreases the remanent magnetization and increases the local magnetic moment to 9.268 μB.

However, Er 4f hybridization in the valence band is presented from −7.5 to 0 eV for the majority DOS close by the Fermi energy in Fig. 2(c). The addition of Co–Er atoms turns BFO to half-metallic character. The Er–Co co-doped BFO has a high concentration at the conduction band minimum due to the contribution of the strong hybridizations principally among Co-3d and Fe-3d states. Also, the majority of the Co 3d state focuses on the Fermi level, which is hybridized with the Er-4f, Er-5p and O-2p states. Er–Co doping enhances the density of unoccupied state of the Fe 3d orbital at the energy of −7.5 eV. The valence band states of BEFCO reduce to about 1.72 eV. Er doping enhances the magnetic of perovskite in experiment, which can also be put down to the super-exchange interaction between Er-4f and Fe-3d elections [21]. The calculated local magnetic moment of BEFCO increases to 4.902 μB. Er 4f and 5p have an effect on ferromagnetic properties, and Co-3d enhances ferroelectric polarization of BFO.

The Lu 4f-states hybridized in valence band with the minority O 2p, Fe 3d and Co 3d states near −3 eV in Fig. 2(d). We can see, from Figs. 2(d) and 3(a), Lu doping affects the Fermi level shift into the top of the valence band, suggesting that the substitution would change the material from a semiconductor to a conductor. Lu-Co doping increases the magnetic moment of BFO to 4.818 μB.

Values of the computed electron localization function (ELF) between atoms of BEFO, BFCO, BErFCO, BLaFCO, BGdFCO and BLuFCO (1 0 1) plane which explain ionic bonding characters are shown in Fig. 3(b). From the contours in graphs, we deduce that the bonds between Fe, Co, Bi and O have covalent character. When rare earth atoms are introduced into BFCO, the bonds between Bi and Co shows a typical covalent and the interaction between Fe and foreign atoms becomes much more intense. The electron density of Er, La, Lu doping samples are major at the O sites and minor at the Fe sites compared to BFCO, the electron density of BGdFCO is minor at the Bi and Fe sites obviously. It is clear that in octahedron cage the Fe ion now alters to more symmetric structures after doping. Er 5p, 4f states, La 4d states, Lu 4f states and Gd 4d states are hybridized with Fe 3d, Bi 6p and O 2p states, which lead to strong actions from the 4f, 4d electrons of rare-earth elements and their participation in bonding. Hence, the oxidation state of the Fe ion slightly increases upon the rare earth-ion substitution for Bi and Co-ion for Fe and $Bi_{0.8}M_{0.2}Fe_{0.9}Co_{0.1}O_3$ (M = La, Gd, Er, Lu) demon-

strate ferroelectric properties (were also confirmed for their crystal anisotropy and permanent dipole moment by Uchida et al. [38]).

3.2. Optical properties

Many physical parameters including the complex dielectric constant $\varepsilon(\omega)$, energy-loss spectrum $L(\omega)$, absorption coefficient $I(\omega)$, optical reflectivity $R(\omega)$, and refractive index $n(\omega)$ have been calculated, in order to investigate the effects of rare-earth elements doping on the optical properties of BCFO. The $\varepsilon(\omega)$ in Eq. (4) describes the linear response of a system which is associated with the electronic structures. The relevance between $\varepsilon(\omega)$ and complex refractive index which describes the propagation of electromagnetic-wave through material can be shown as below [39]

$$\varepsilon(\omega) = \varepsilon_1(\omega) + i\varepsilon_2(\omega), \tag{4}$$

$$N(\omega) = n(\omega) + ik(\omega), \tag{5}$$

$$\varepsilon(\omega) = N^2(\omega), \tag{6}$$

where $\varepsilon_1(\omega)$ is the real part of $\varepsilon(\omega)$ following from the Kramer–Kroing transformation. The imaginary part $\varepsilon_2(\omega)$ which is connected to the band structure can be got by gathering all transitions from occupied states to unoccupied electric states [40]. We can obtain $\varepsilon_1(\omega)$ by

$$\varepsilon_1(\omega) = 1 + \frac{2}{\pi}\int_0^\infty \frac{\varepsilon_2(\omega')\omega' d\omega'}{\omega'^2 - \omega^2}. \tag{7}$$

$\varepsilon_2(\omega)$ obeys the following relation:

$$\varepsilon_2(\omega) = \left(\frac{Ve^2}{2\pi\hbar m^2\omega^2}\right)\int d^3k \sum_{nn'} |\langle kn|p|kn'\rangle|^2 \times f(kn)(1 - f(fn'))\delta(E_{kn} - E_{kn'} - \hbar\omega). \tag{8}$$

$\hbar\omega$ is the energy of the incident electron, P is the momentum operator, $-i\hbar\frac{\partial}{\partial x}|kn\rangle$ is the eigenfunction with eigenvalue E_{kn}, $f(kn)$ is the Fermi distribution function.

Then $L(\omega)$, $I(\omega)$, $R(\omega)$, $n(\omega)$ can be given via the following expressions [41]

$$L(\omega) = \frac{\varepsilon_2(\omega)}{\varepsilon_1^2(\omega) + \varepsilon_2^2(\omega)}, \tag{9}$$

$$I(\omega) = \sqrt{2}\omega\left[\sqrt{\varepsilon_1^2(\omega) + \varepsilon_2^2(\omega)} - \varepsilon_1(\omega)\right]^{1/2}, \tag{10}$$

$$R(\omega) = \left|\frac{\sqrt{\varepsilon(\omega)} - 1}{\sqrt{\varepsilon(\omega)} + 1}\right|^2, \tag{11}$$

$$n(\omega) = \frac{1}{\sqrt{2}}\left[\sqrt{\varepsilon_1^2(\omega) + \varepsilon_2^2(\omega)} + \varepsilon_1(\omega)\right]^{1/2}. \tag{12}$$

The real and imaginary part curves of BFO, BEFO, BFCO, BEFCO, BLaFCO, BGdFCO and BLuFCO are presented in Fig. 4(a). While the value of energy is zero, the static dielectric function is equal to 7.6, 8.7, 9.0, 7.0, 7.4, 9.2 and 10.5 for BFO, BEFO, BFCO, BEFCO, BLaFCO, BGdFCO and BLuFCO respectively in this work.

The reason that three peaks in the imaginary part of BFO (5.0, 7.2 and 13.4 eV) can attribute to the transformation of O 2p electron (O 2p → Fe 3d and O 2p → Bi 6p) [42,43]. For the BEFO sample, there is only the imaginary part of BEFO reveals one strong peak with a weak shoulder peak which owes to the transitions from O 2p valance bands to the Fe 3d or Er 4f conduction bands at 4.5 eV. BFCO, BEFCO and BLaFCO present similar three peaks at 2.5, 7.2 and 13.4 eV which are credited to the transitions from O 2p to the Er 4f and to the Co 3d. Besides, the extra peak at 20 eV of La originates from O 2 s and La 4d states in the valance bands to Bi 6p states in the conduction bands. $\varepsilon_2(\omega)$ of BGdFCO has two

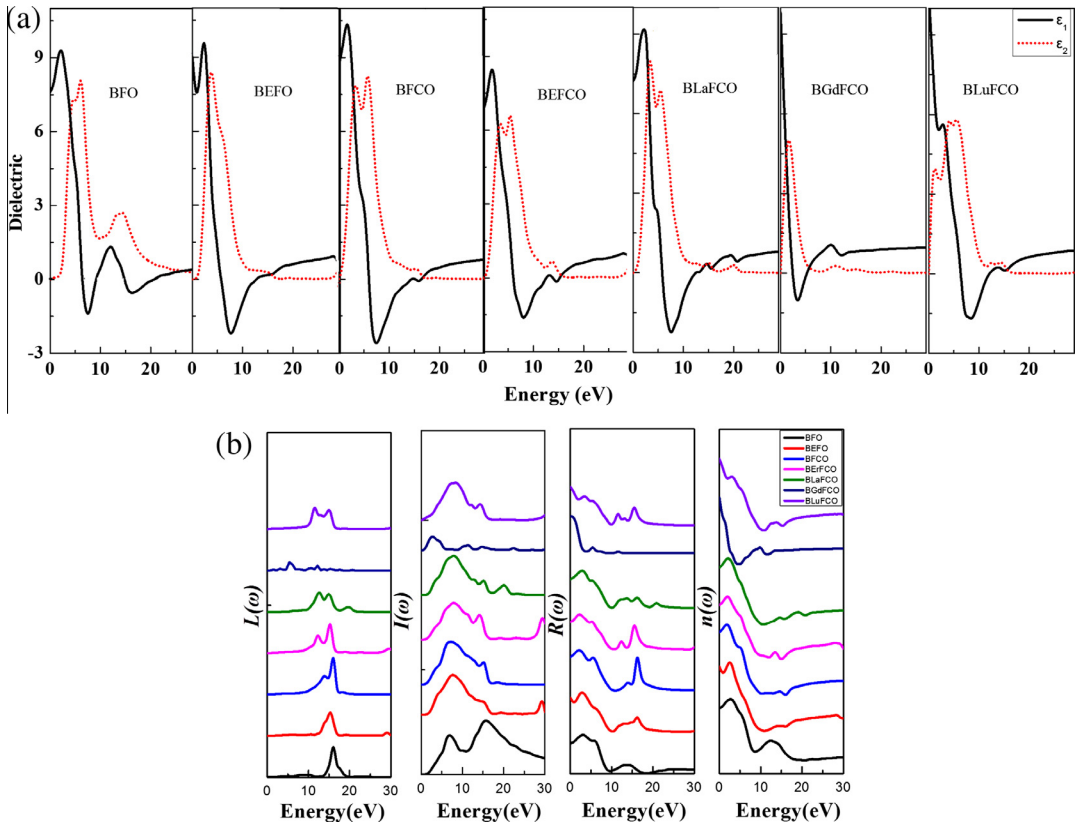

Fig. 4. (a) Calculated the real part $\varepsilon_1(\omega)$ and imaginary part $\varepsilon_2(\omega)$ curves of complex dielectric constant $\varepsilon(\omega)$ and (b) other optical properties (energy-loss spectrum $L(\omega)$, absorption coefficient $I(\omega)$, optical reflectivity $R(\omega)$, and (h) refractive index $n(\omega)$) for BFO, BEFO, BFCO, BEFCO, BLaFCO, BGdFCO and BLuFCO.

peaks, the peak at 2.5 eV results from the transition of O 2p states into Fe 3d states in the conduction bands, the peak at 10.5 eV is mainly due to the transition of Co 3d states in the middle valence bands to Bi 6p states. There are 5 peaks located at 2.5, 5.0, 7.4, 12.5 and 15.0 eV for Lu-doped BFCO, which originate from O-2p → Co-3d, O-2p → Fe-3d, Lu-4d → Fe-3d, Bi-6p → Fe-3d and Bi-6p to the upper conduction band. It can be seen that the 4f electronic of rare-earth elements especially Lu ($4f^{14}$) and Gd ($4f^{7}$) have obvious effects on the dielectric constant.

Fig. 4(b) shows a comparison of BFO, BEFO, BFCO, BEFCO, BLaFCO, BGdFCO and BLuFCO for the energy loss spectrum $L(\omega)$, absorption coefficient $I(\omega)$, reflectivity $R(\omega)$, and refractive index $n(\omega)$ in the range of 0–30 eV. The peaks of $L(\omega)$ which are corresponding to the abrupt reduction in the $R(\omega)$ toward the small energy side for Er, La, Gd and Lu doping. In Fig. 4(b), the absorption edge of BEFCO, BLaFCO, BGdFCO and BLuFCO Can be signed as 1.5 eV, 0.5 eV, 0.2 eV and 0 eV respectively, corresponding to their band gap. From the PDOS of BEFCO in Fig. 2(c), we can conclude that the first absorption peak among 8.5–10.0 eV is unconspicuous (forming by the Co 3d → Bi 6p) while the second peak around 15.0 eV is distinct (due to the overlap of Er-5p orbit with the 2p orbital of O). The similar results can be obtained for BLaFCO, BGdFCO and BLuFCO. In the region 10–20 eV, the reflection of calculated $n(\omega)$ is strong and have several peaks, while the refraction of $R(\omega)$ have opposite change tendency and become weak. It can be found that lines of refractive index $n(\omega)$ have same trend with lines of $\varepsilon_1(\omega)$ for $Bi_{0.8}M_{0.2}Fe_{0.9}Co_{0.1}O_3$ (M = La, Gd, Er, Lu) from Fig. 4(b).

4. Conclusions

In summary, the effect of La, Gd, Er, Lu doping on the variations of the electronic, magnetic and optical for $BiFe_{0.9}Co_{0.1}O_3$ were studied by using the first-principles. It has been noted that the calculated DOS illustrated hybridization between 4f and 4d electrons of La, Gd, Er, Lu ions and 2p electrons of O^{2-} ion, 6p electrons of Bi^{+} ion, 3d electrons of Fe^{3+} ion and Co^{3+} ion. Analysis of DOS and band structure of BLuFCO and BGdFCO reveal that Lu and Gd elements intercalate into $BiFe_{0.9}Co_{0.1}O_3$ transform the semiconductor to be conductor. The total magnetic moments are 4.895, 9.268, 4.902 and 4.818 μB for La, Gd, Er and Lu doping, respectively. The 4f electronic of rare-earth elements especially Lu ($4f^{14}$) and Gd ($4f^{7}$) have obvious effects on the dielectric constant $\varepsilon(\omega)$. The absorption spectra also show an advanced optical response in the visible range for BLuFCO and BGdFCO, and their optical transitions originate mainly from O 2p valance bands to the Fe 3d or Lu/Gd 4f conduction bands. These results suggest that BLuFCO and BGdFCO thin films could be considered as potential materials for photovoltaic devices.

Acknowledgements

We acknowledge the financial support from the National Basic Research Program of China (2014CB648300 and 2015CB932203), the Ministry of Education of China (No. IRT1148), National Synergistic Innovation Center for Advanced Materials (SICAM), Natural Science Foundation of Jiangsu Province, China (BM2012010), the Project Funded by the Priority Academic Program Development of Jiangsu Higher Education Institutions (PAPD, YX03001), the National Natural Science Foundation of China (51172110, 51372119, 61377019 and 61136003).

Appendix A. Supplementary material

Supplementary data associated with this article can be found, in the online version, at http://dx.doi.org/10.1016/j.comptc.2016.03.001.

References

[1] Y.W. Fang, H.C. Ding, W.Y. Tong, W.J. Zhu, X. Shen, S.J. Gong, X.G. Wan, C.G. Duan, First-principles studies of multiferroic and magnetoelectric materials, Sci. Bull. 60 (2) (2015) 156–181.
[2] W. Kleemann, C. Binek, Multiferroic and magnetoelectric materials, Nature 442 (104) (2006) 759–765.
[3] K.F. Wang, J.M. Liu, Z.F. Ren, Multiferroicity: the coupling between magnetic and polarization orders, Adv. Phys. 58 (4) (2009) 321–448.
[4] Y.J. Zhang, J.F. Hu, F. Gao, H. Liu, H.W. Qin, Ab initio calculation for vacancy-induced magnetism in ferroelectric $Na_{0.5}Bi_{0.5}TiO_3$, Comput. Theor. Chem. 967 (2011) 284–288.
[5] K.S. Kumar, J. Ayyappan, C. Venkateswaran, Structural, magnetic and electrical properties of $BiFeO_3$ co-substituted with Pr–Mn, Mater. Res. Bull. 65 (7) (2015) 224–230.
[6] J. Wang, J.B. Neaton, H. Zheng, V. Nagarajan, S.B. Ogale, B. Liu, D. Viehland, V. Vaithyanathan, D.G. Schlom, U.V. Waghmare, N.A. Spaldin, K.M. Rabe, M. Wuttig, R. Ramesh, Epitaxial $BiFeO_3$ multiferroic thin film heterostructures, Science 299 (5613) (2003) 1719–1722.
[7] C. Gustau, F.S. James, Physics and applications of bismuth ferrite, Adv. Mater. 21 (2009) 2463–2485.
[8] M. Rangi, A. Agarwal, S. Sanghi, R. Singh, S.S. Meena, A. Das, Crystal structure and magnetic properties of $Bi_{0.8}A_{0.2}FeO_3$ (A = La, Ca, Sr, Ba) multiferroics using neutron diffraction and Mossbauer spectroscopy, AIP Adv. 4 (2014) 87–121.
[9] G.Q. Tan, Y.Y. Luo, G.H. Dong, W. L Liu, H.J. Ren, A. Xia, A comparative study on the magnetic and electrical properties of $Bi_{0.89}Tb_{0.11}FeO_3$ and $Bi_{0.89}Tb_{0.11}FeO_3$/$CoFe_2O_4$ multiferroic thin films, J. Alloys Compd. 623 (2015) 243–247.
[10] S.A. Prosandeev, D.D. Khalyavin, I.P. Raevski, A.N. Salak, N.M. Olekhnovich, A.V. Pushkarev, Y.V. Radyush, Complex antipolar $\sqrt{2} \times 4 \times 2\ \sqrt{2}$ structure with Pnma symmetry in $BiFeO_3$ and $BiFe_{1/2}Sc_{1/2}O_3$: first-principles calculations, Phys. Rev. B 90 (2014) 54–60.
[11] F. Yan, M.O. Lai, L. Lu, Enhanced multiferroic properties and valence effect of Ru-doped $BiFeO_3$ thin films, J. Phys. Chem. C 114 (2010) 6994–6998.
[12] X. Yan, G.Q. Tann, W.L. Liu, H.J. Ren, A. Xia, Structural, electric and magnetic properties of Dy and Mn co-doped $BiFeO_3$ thin films, Ceram. Int. 41 (2015) 3202–3207.
[13] Q. Xu, M. Sobhan, F. Anariba, J.W. Chye, C.P. Wu, Transition metal-doped BiFeO3 nanofibers: forecasting the conductivity limit, Phys. Chem. Chem. Phys. 16 (2014) 23089–23095.
[14] A. Singh, A. Gupta, R. Chatterjee, Enhanced magnetoelectric coefficient (α) in the modified $BiFeO_3$–$PbTiO_3$ system with large La substitution, Appl. Phys. Lett. 93 (2) (2008) 022902–022903.
[15] K.S. Nalwa, G.J. Ashish, Magnetic and electrical properties in Sm-doped bismuth ferrite, J. Appl. Phys. 103 (2008) 044101–044106.
[16] J. Liu, H.M. Deng, H.Y. Cao, X.Z. Zhai, J.H. Tao, L. Sun, P.X. Yang, Junhao Chu, Influence of rare-earth elements doping on structure and optical properties of $BiFeO_3$ thin films fabricated by pulsed laser deposition, Appl. Surf. Sci. 307 (2014) 543–547.
[17] J. Raya, A.K. Biswala, S. Acharyaa, V. Ganesanb, D.K. Pradhana, P.N. Vishwakarma, Effect of Co substitution on the magnetic properties of $BiFeO_3$, J. Magn. Magn. Mater. 324 (2012) 4084–4089.
[18] Q.Y. Xu, H.F. Zai, D. Wu, T. Qiu, M.X. Xu, The magnetic properties of Bi$(Fe_{0.95}Co_{0.05})O_3$ ceramics, Appl. Phys. Lett. 95 (2009) 112510–112513.
[19] X. Xue, G.Q. Tan, W.L. Liu, H.F. Hao, H.J. Ren, Structural, electrical, and magnetic properties of multiferroic $Bi_{1-x}Gd_xFe_{0.97}Co_{0.03}O_3$ thin films, J. Alloys Compd. 622 (2015) 477–482.
[20] W.W. Mao, X.F. Wang, Y.M. Han, X.A. Li, Y.T. Li, Y.F. Wang, Y.W. Ma, X.M. Feng, T. Yang, J.P. Yang, W. Huang, Effect of Ln (Ln = La, Pr) and Co co-doped on the magnetic and ferroelectric properties of $BiFeO_3$ nanoparticles, J. Alloys Compd. 584 (2014) 520–523.
[21] Y.M. Han, W.W. Mao, C.Y. Quan, X.F. Wang, J.P. Yang, T. Yang, X.A. Li, W. Huang, Enhancement of magnetic and ferroelectric properties of $BiFeO_3$ by Er and transition element (Mn, Co) co-doping, Mater. Sci. Eng. B 188 (2014) 26–30.
[22] P. Singh, A. Roy, A. Garg, R. Prasad, Effect of isovalent non-magnetic Fe-site doping on the electronic structure and spontaneous polarization of $BiFeO_3$, J. Appl. Phys. 117 (2015) 184104.
[23] H.H. Nguyen, T.H. Ngo, T.Y. Kim, Tuning magnetic properties of $BiFeO_3$ thin films by controlling rare-earth doping: experimental and first-principles studies, J. Phys. Chem. C 119 (2015) 14351–14357.
[24] D. Dalhyun, W.K. Jin, Electrical properties in lanthanides substituted $(Bi_{0.9}A_{0.1})(Fe_{0.975}Co_{0.025})O_{3-\delta}$(A = La, Eu, Gd) thin films, J. Korean Phys. Soc. 61 (2012) 1409–1412.
[25] G. Kresse, J. Furthmüller, Efficiency of ab-initio total energy calculations for metals and semiconductors using a plane-wave basis set, Comput. Mater. Sci. 6 (1996) 15–50.
[26] G. Kresse, J. Furthmüller, Efficient iterative schemes for ab initio total-energy calculations using a plane-wave basis set, Phys. Rev. B 54 (1996) 11169–11170.
[27] J.P. Perdew, K. Burke, M. Ernzerhof, Generalized gradient approximation made simple, Phys. Rev. Lett. 78 (1997) 1396–1397.
[28] Z.H. Yang, Y. Pei, X.Y. Wang, L. Liu, X.P. Su, First principles study on the structural, magnetic and electronic properties of Co-doped FeF_3, Comput. Theor. Chem. 980 (2012) 44–48.
[29] K. Chakrabarti, B. Sarkar, V.D. Ashok, S.S. Chaudhuri, S.K. De, Enhanced magnetic and dielectric behavior in Co doped $BiFeO_3$ nanoparticles, J. Magn. Magn. Mater. 381 (2015) 271–277.

[30] T. Jia, H. Wu, G.R. Zhang, X.L. Zhang, Y. Guo, Z. Zeng, H.Q. Lin, Ab initio study of the giant ferroelectric distortion and pressure-induced spin-state transition in $BiCoO_3$, Phys. Rev. B 83 (2011) 174433.
[31] H.V. Aggelen, Single-particle energies and density of states in density functional theory, Mol. Phys. 113 (2015) 2018–2025.
[32] C. Nardini, R. Nerattini, L. Casetti, Density of states of the XY model: an energy landscape approach, Phys. A 420 (2015) 229–245.
[33] S.Y. Davydov, On the density of states of disordered epitaxial graphene, Semiconductors 49 (2015) 615–620.
[34] K.G. Yang, Y.L. Zhang, S.H. Yang, B. Wang, Structural, electrical, and magnetic properties of multiferroic $Bi_{1-x}La_xFe_{1-y}Co_yO_3$ thin films, J. Appl. Phys. 107 (2010) 124109.
[35] N. Gao, C.Y. Quan, Y.H. Ma, Y.M. Han, Z.L. Wu, W.W. Mao, J. Zhang, J.P. Yang, X. A. Li, W. Huang, Experimental and first principles investigation of the multiferroics $BiFeO_3$ and $Bi_{0.9}Ca_{0.1}FeO_3$: structure, electronic, optical and magnetic properties, Phys. B 481 (2016) 45–52.
[36] J.W. Kim, S.S. Kim, H.J. Kim, W.J. Kim, C.M. Raghavan, D. Do, M.H. Lee, T.K. Song, M.H. Kim, Enhance ment of ferroelectri city in gadolinium (Gd) and transition metal (Ni Co, Cr) co-doped $BiFeO_3$ thin films via a chemical solution deposition technique, J. Electroceram. 30 (2013) 13–18.
[37] A. Ablat, R. Wu, M. Mamat, J. Li, E. Muhemmed, C. Si, R. Wu, J. Wang, H.J. Qian, K. Ibrahim, Structural analysis and magnetic properties of Gd doped $BiFeO_3$ ceramics, Ceram. Int. 40 (2014) 14083–14089.
[38] H. Uchida, R. Ueno, H. Funakubo, S. Koda, Crystal structure and ferroelectric properties of rare-earth substituted $BiFeO_3$ thin films, J. Appl. Phys. 100 (2006) 014106.
[39] J. Tauc, T.A. Scott, Optical properties of solids, Phys. Today 1 (2009) 105–107.
[40] K. Liu, H.Q. Fan, P.R. Ren, C. Yang, Structural, electronic and optical properties of $BiFeO_3$ studied by first-principles, J. Appl. Compd. 509 (2011) 1901–1905.
[41] C.A. Draxl, J.O. Sofo, Linear optical properties of solids within the full-potential linearized augmented planewave method, Comput. Phys. Comm. 175 (2006) 1–2.
[42] K.A. McDonnell, N. Wadnerkar, N.J. English, M. Rahman, D. Dowlin, Photo-active and optical properties of bismuth ferrite ($BiFeO_3$): an experimental and theoretical study, Chem. Phys. Lett. 572 (2013) 78–84.
[43] D. Li, F.R. Ling, First-principles calculation of structural, electronic, and optical properties of wurtzite–stannite Cu_2MgSi $(S_xSe_{1-x})_4$ alloys, Comput. Theor. Chem. 1074 (2015) 163–167.